CONTROL OF THE PHOTOVOLTAIC EMULATOR USING FUZZY LOGIC BASED RESISTANCE FEEDBACK AND BINARY SEARCH

RAZMAN BIN AYOP

A thesis submitted in fulfilment of the
requirement for the award of degree of
Doctor of Philosophy

School of Electrical Engineering
Faculty of Engineering
Universiti Teknologi Malaysia

NOVEMBER 2018

DEDICATION

To my Family, for their patience, support, love and for enduring the ups and downs during the completion of this thesis.

ACKNOWLEDGEMENT

I would like to express my deepest gratitude to my supervisor, Ir. Dr. Tan Chee Wei for his outstanding support and excellent supervision. This research would not have been successful without his valuable guidance, enthusiastic help as well as constructive criticisms throughout the research.

My whole appreciation to the lecturer at School of Electrical Engineering, University Teknologi Malaysia especially Dr. Norjulia Mohamad Nordin. I also would like to thank the Power Electronic Laboratory technicians, Mr. Shafie Nordin and Mr. Yusuf Jamil, for your help and supports during my research. Also, thanks to Nor Akmal Rai, Normazlina Mat Isa, Himadry Shekhar Das, Mohamed Salem, Megat Azahari Chulan, Nur Huda Ramlan, Izni Mustafar, Hairol Jaffar, AbdulHakeem D. Mohammed, Rozana Alik and all those who had helped me in one-way or other during my research.

Special thanks to my beloved parents for their wisdom and continuous support and guidance throughout my PhD journey. Thank you for your encouragement, continuous support and your understanding throughout my PhD journey.

I would like to thank Ministry of Higher Education for granting my scholarship. Last but not least, to the Ministry of Higher Education (MOHE) for providing the research grants and to the Universiti Teknologi Malaysia for allowing me to use the facilities during my research is greatly appreciated and without it, this research could not have been carried out.

ABSTRACT

Photovoltaic (PV) emulator is a power supply that produces similar current-voltage (I-V) characteristics as the PV module. This device simplifies the testing phase of PV systems under various conditions. The essential part of the PV emulator (PVE) is the control strategy. Its main function is to determine the operating point based on the load of the PVE. The direct referencing method (DRM) is the widely used control strategy due to its simplicity. However, the main drawback of DRM is that the output voltage and current oscillate due to the inconsistent operating point under fixed load. This thesis proposes an improved and robust control strategy named resistance feedback method (RFM) that yields consistent operating point under fixed load, irradiance and temperature. The RFM uses the measured voltage and current to determine the load of the PVE in order to identify the accurate operating point instantaneously. The conventional PV models include the I-V and voltage-current PV model. These PV models are widely used in various control strategies of PVE. Nonetheless, the RFM requires a modified PV model, the current-resistance (I-R) PV model, where the mathematical equation is not available. The implementation of the I-R PV model using the look-up table (LUT) is feasible, but it requires a lot of memory to store the data. A mathematical equation based I-R PV model computed using the binary search method is proposed to overcome the drawback of the LUT. The RFM consists of the I-R PV model and the closed-loop buck converter. In this work, the RFM is investigated with two different controllers, namely the proportional-integral (PI) and fuzzy logic controllers. The RFM using the PI controller (RFMPI) and the RFM using the fuzzy logic controller (RFMF) are tested with resistive load and maximum power point tracking (MPPT) boost converter. The perturb and observe algorithm is selected for the MPPT boost converter. In order to properly design the boost converter for the MPPT application, the sizing of the passive components is proposed, derived and confirmed through simulation. This derivation allows adjustment on the output voltage and current ripple of the PVE when connected to the MPPT boost converter. The simulation results of the proposed control strategies are benchmarked with the conventional DRM. To validate the simulation results, all controllers are implemented using dSPACE ds1104 rapid prototyping hardware platform. The RFM computes an operating point of the PVE at 20% faster than the DRM. The generated output PVE voltage and current using RFMPI and the RFMF are up to 90% more accurate compared to the DRM. The efficiency of the PVE is beyond 90% when tested under locus of maximum power point. In transient analysis, the settling time of RFMF is faster than the RFMPI. In short, the proposed RFMF is robust, accurate, quick respond and compatible with the MPPT boost converter.

ABSTRAK

Pelagak fotovolta (PV) ialah sebuah bekalan kuasa yang menghasilkan ciri-ciri arus-voltan (I-V) yang serupa dengan modul PV. Peranti ini dapat memudahkan fasa pengujian sistem PV pada pelbagai keadaan. Bahagian penting dalam pelagak PV (PVE) ialah strategi kawalan. Fungsi utamanya adalah untuk menentukan titik pengoperasian berdasarkan beban pada PVE. Kaedah rujukan langsung (DRM) merupakan strategi kawalan yang digunakan secara meluas kerana ianya mudah. Namun, kelemahan utama DRM ialah voltan dan arus keluarannya berayun disebabkan oleh titik pengoperasian yang tidak konsisten pada beban tetap. Tesis ini mencadangkan strategi kawalan yang diperbaik dan teguh yang dinamakan kaedah suap balik perintang (RFM) yang menghasilkan titik pengoperasian yang konsisten pada beban, kesinaran dan suhu yang tetap. RFM menggunakan voltan dan arus yang diukur untuk menentukan beban pada PVE bagi menentukan titik pengoperasian yang tepat secara serta-merta. Model-model PV lazim yang digunakan ialah model PV I-V dan voltan-arus. Model-model PV ini digunakan secara meluas dalam pelbagai strategi kawalan untuk PVE. Walau bagaimanapun, RFM memerlukan model PV yang diubahsuai, iaitu model PV arus-perintang (I-R), yang persamaan matematiknya belum diterbitkan. Pelaksanaan model PV I-R menggunakan jadual carian (LUT) boleh dilaksanakan, tetapi ianya memerlukan banyak ingatan untuk menyimpan data. Satu persamaan matematik berdasarkan model PV I-R yang diselesaikan menggunakan kaedah carian gelintar perduaan, dicadangkan untuk mengatasi kelemahan LUT. RFM terdiri daripada model PV I-R dan penukar menurun gelung tertutup. Dalam tesis ini, RFM diuji dengan dua pengawal yang berbeza, iaitu pengawal kamiran-perkadaran (PI) dan pegawal logik kabur. RFM menggunakan pengawal PI (RFMPI) dan RFM menggunakan pengawal logik kabur (RFMF) diuji menggunakan beban perintang dan penukar menaik penjejakan titik kuasa maksimum (MPPT). Algoritma usik dan perhati dipilih untuk penukar menaik MPPT. Bagi mereka bentuk penukar menaik secara betul, pensaizan komponen pasif dicadangkan, diterbitkan dan disahkan melalui simulasi. Terbitan ini membolehkan pelarasan riak voltan dan riak arus keluaran PVE apabila disambung pada penukar menaik MPPT. Keputusan simulasi bagi strategi-strategi kawalan yang dicadangkan itu dibandingkan dengan DRM lazim. Bagi mengesahkan keputusan simulasi, kesemua pengawal dilaksanakan menggunakan platform perkakasan prototaip pantas dSPACE ds1104. RFM dapat mengira satu titik pengoperasian bagi PVE pada 20% lebih pantas berbanding dengan DRM. Voltan dan arus keluaran yang dihasilkan oleh PVE mengunakan RFMPI dan RFMF adalah mencecah 90% lebih tepat berbanding dengan DRM. Kecekapan PVE melebihi 90% apabila diuji pada lokus titik kuasa maksimum. Untuk analisis fana, masa enapan bagi RFMF adalah lebih pantas berbanding dengan RFMPI. Pendek kata, RFMF yang dicadangkan ialah teguh, tepat, cepat bertindak balas dan serasi dengan penukar menaik MPPT.

TABLE OF CONTENTS

TITLE		PAGE
	DECLARATION	ii
	DEDICATION	iii
	ACKNOWLEDGEMENT	iv
	ABSTRACT	v
	ABSTRAK	vi
	TABLE OF CONTENTS	vii
	LIST OF TABLES	xii
	LIST OF FIGURES	xiv
	LIST OF ABBREVIATIONS	xx
	LIST OF SYMBOLS	xxi
	LIST OF APPENDICES	xxiv
CHAPTER 1	**INTRODUCTION**	**1**
1.1	Background of the Study	1
1.2	Problem Statement	4
1.3	Research Objectives	7
1.4	Research Methodology	7
1.5	Research Contribution	8
1.6	Scope of the Study	9
1.7	Thesis Organization	10
CHAPTER 2	**OVERVIEW OF PHOTOVOLTAIC EMULATOR**	**13**
2.1	Photovoltaic Model	14
	2.1.1 Types of Photovoltaic Model	15
	2.1.1.1 Parameter Extraction	18
	2.1.1.2 Features of Photovoltaic Model	19
	2.1.1.3 Comparison of Photovoltaic Electrical Circuit Model	20
	2.1.2 Implementation of Photovoltaic Model	21

2.2 Power Converter 25
2.2.1 Types of Power Converter 25
2.2.1.1 Non-Galvanic Isolation Converter 25
2.2.1.2 Galvanic Isolation Converter 26
2.2.1.3 Interleaved Converter 27
2.2.1.4 Synchronous Converter 28
2.2.1.5 Resonant Converter 29
2.2.1.6 Linear Regulator 29
2.2.1.7 Programmable Power Supply 30
2.2.2 Controllers for Power Converter 30
2.2.2.1 Small Signal Analysis 31
2.2.2.2 Proportional-Integral-Derivative Controller 33
2.2.2.3 Fuzzy Controller 35
2.2.2.4 Other Controllers 36
2.3 Control Strategy 37
2.3.1 Direct Referencing Method 37
2.3.2 Hybrid-Mode Control Method 39
2.3.3 Indirect Referencing Method 41
2.3.4 Resistance Comparison Method 41
2.3.5 Analogue Based Control Strategy 43
2.3.6 Analysis and Discussions on Control Strategies 45
2.4 Photovoltaic Emulator Testing 48
2.5 Summary 50

CHAPTER 3 DESIGN OF PHOTOVOLTAIC EMULATOR 51
3.1 Photovoltaic Model 51
3.1.1 Theoretical Parameters of PV Model 51
3.1.2 Current-Resistance Photovoltaic Model 54
3.1.3 Newton-Raphson Method 54
3.1.4 Binary Search Method 55
3.2 Power Converter 58
3.2.1 Buck Converter 59
3.2.2 State-Space Averaging 62
3.2.3 Proportional-Integral Controller 65

3.2.4 Fuzzy Controller 67
3.3 Control Strategy 73
3.3.1 Direct Referencing Method 74
3.3.2 Resistance Feedback Method 75
3.3.2.1 Proportional-Integral Based Controller 76
3.3.2.2 Fuzzy Based Controller 77
3.4 Maximum Power Point Tracking Converter 78
3.4.1 Boost Converter Derivation 79
3.4.1.1 Maximum Power Point Resistance 81
3.4.1.2 Output Resistance 83
3.4.1.3 Inductance 86
3.4.1.4 Input Capacitance 89
3.4.1.5 Output Capacitance 91
3.4.1.6 Design Procedure 92
3.4.2 Perturb and Observe Algorithm 94
3.5 Summary 95

CHAPTER 4 SIMULATION RESULTS AND DISCUSSIONS 97
4.1 Convergence of the Photovoltaic Model 98
4.2 Robustness of the Control Strategy 99
4.2.1 Direct Referencing Method 100
4.2.2 Resistance Feedback Method 103
4.3 Accuracy of the Photovoltaic Emulator 105
4.3.1 Accuracy of the Photovoltaic Model 106
4.3.2 Accuracy of the Control Strategy 109
4.4 Transient Response of the Photovoltaic Emulator 114
4.4.1 Start-Up Test 115
4.4.2 Load Test 118
4.4.3 Irradiance Test 120
4.4.4 Temperature Test 121
4.5 Efficiency of the Photovoltaic Emulator 122
4.6 Accuracy of the Maximum Power Point Tracking Boost Converter Derivation 124
4.6.1 Duty Cycle 124

4.6.2 Ripple Factor 125
4.6.2.1 Inductor Current 126
4.6.2.2 Input Capacitor Voltage 128
4.6.2.3 Output Capacitor Voltage 129
4.7 Maximum Power Point Tracking Integration 131
4.8 Summary 134

CHAPTER 5 HARDWARE DESIGN AND EXPERIMENTAL VALIDATION 137

5.1 Hardware Implementation 137
5.1.1 Power Converter 138
5.1.2 dSPACE ds1104 Hardware Platform 140
5.1.3 Gate Driver 141
5.1.4 Current and Voltage Sensor Circuit 142
5.1.5 Amplifier Circuit 144
5.2 Measurement and Analysis 145
5.3 Computation of the Photovoltaic Emulator 147
5.3.1 Computation of the Photovoltaic Model 148
5.3.2 Computation of the Operating Point 149
5.4 Robustness of the Control Strategy 150
5.5 Accuracy of the Control Strategy 155
5.6 Transient Response of the Photovoltaic Emulator 156
5.6.1 Start-Up Test 157
5.6.2 Load Test 159
5.6.3 Irradiance Test 163
5.7 Efficiency of the Photovoltaic Emulator 166
5.8 Maximum Power Point Tracking Integration 167
5.9 Summary 169

CHAPTER 6 CONCLUSION AND FUTURE WORK **171**

6.1 Conclusion 171

6.1.1 Resistance Feedback Method 171

6.1.2 Current-Resistance Photovoltaic Model 172

6.1.3 Fuzzy Error Compensator 173

6.1.4 Design of Boost Converter for Maximum Power Point Tracking 173

6.2 Future Work 174

REFERENCES **177**

Appendices A - E 189 - 211

LIST OF TABLES

TABLE NO.	TITLE	PAGE
Table 2.1	Summary of the advantages and disadvantages of the PV model implementation method for the PVE	24
Table 3.1	The parameters of the Ameresco Solar80 J-BPV module	52
Table 3.2	The parameters of the designed buck converter for the PVE	62
Table 3.3	The proportional and integral gains for various types of controller for the buck converter	66
Table 3.4	The fuzzy rule matrix	72
Table 3.5	The design parameters required to calculate the components of the MPPT boost converter	80
Table 3.6	The pre-defined boundaries of the MPPT output resistance	84
Table 3.7	The calculated values of the components required for the ideal and nonideal MPPT boost converter	85
Table 3.8	The summary of the design of the PVE using the DRM, the RFMPI and the RFMF	96
Table 4.1	The data samples of the t_s (ms) correspond to Figure 4.11.	115
Table 4.2	Summary of the performance characteristics of the PVE among the DRM, the RFMPI and the RFMF	135
Table 5.1	The parameters of the sensor and amplifier circuit	142
Table 5.2	The equipment, the measurements and the analysis involved in the experimental validation	147
Table 5.3	The number of iterations and the convergence time to converge the PV model	149
Table 5.4	The number of iterations and the convergence time to converge an operating point	150

Table 5.5 The experimental results of the robustness of the control strategy and the corresponding reference voltage and current 151

Table 5.6 The simulation and experimental PVE’s efficiency at MPP 167

Table 5.7 Performance comparison of the PVE between the simulation and experiment results 170

LIST OF FIGURES

FIGURE NO.	TITLE	PAGE
Figure 1.1	The three components of the PVE system	3
Figure 1.2	The influence of the three components in the PVE system toward the performance of the PVE	3
Figure 1.3	The area of the constant current and voltage regions in the PV I-V characteristic curve	6
Figure 1.4	The contribution categories based on the components of the PVE system	9
Figure 2.1	The overview of the three components of the PVE system	13
Figure 2.2	The overview of the PV model in the PVE application	15
Figure 2.3	The electrical circuit model of PV cell, (a) the single diode model (1D2R model) and (b) the double diode model (2D2R model)	16
Figure 2.4	The electrical circuit model of the simplified single diode model, a) the single diode model with a series resistor (1D1R model), b) the ideal single diode model (1D model)	18
Figure 2.5	The schematic circuit of the two phase interleaved buck converter	27
Figure 2.6	The closed-loop control power converter using the PID controller for a) the voltage-mode control and b) the current-mode control	34
Figure 2.7	The block diagram of the fuzzy controller	35
Figure 2.8	The control strategy of the PVE	37
Figure 2.9	The DRM integrated in the PVE, a) using the current mode control, b) using the voltage-mode control	38
Figure 2.10	The block diagram shows the control strategy concept of the resistance comparison method	42

Figure 2.11 The resistance line method used to determine the I_{ref} and V_{ref} for the PVE 43

Figure 3.1 The comparison between the PV model and the manufacturer's I-V characteristic data of Ameresco Solar80J-BPV module under various irradiances. a) The I-V characteristic curve. b) The P-V characteristic curve 53

Figure 3.2 The implementation of the binary search method to solve the I-R PV characteristic equation 57

Figure 3.3 The circuit schematic of the buck converter with the internal resistance 59

Figure 3.4 The area of operation for the PVE using buck converter and the corresponding range of output resistance 60

Figure 3.5 The equivalent circuit of the buck converter when the MOSFET is turned on and the diode is reversed biased 63

Figure 3.6 The equivalent circuit of the buck converter when the MOSFET is turned off and the diode is forward biased 63

Figure 3.7 The block diagram of the closed-loop current-mode control buck converter using the PI controller 65

Figure 3.8 The bode plot of the open-loop buck converter with the PI controller at 5 Ω and 90 Ω output resistance for the closed-loop stability analysis 66

Figure 3.9 The reference and output current of the DRM at high R_o 67

Figure 3.10 The block diagram of the current-mode control power converter using the proposed fuzzy controller. b) The flowchart to calculate new $D_{(k)}$ 69

Figure 3.11 The input and output membership functions of the proposed fuzzy controller. a) *State*. b) R_o. c) K_e 71

Figure 3.12 a) The two dimensional and b) the three-dimensional surface corresponding to the membership function and the rules 73

Figure 3.13 The block diagram of the conventional DRM using the buck converter 74

Figure 3.14	The estimation of the retuned K_i for the DRM	75
Figure 3.15	The block diagram of the proposed RFM	76
Figure 3.16	The block diagram of the proposed RFMPI using the buck converter	77
Figure 3.17	The block diagram of the proposed RFMF using the buck converter	78
Figure 3.18	The schematic circuit of the boost converter with the internal resistance and the P&O MPPT controller	79
Figure 3.19	The schematic circuit of the ideal MPPT boost converter and the representation of the R_{mp}	81
Figure 3.20	The I-V characteristic curves of a PV module under different irradiances: the representation of the MPP as the R_{mp}	82
Figure 3.21	The inductor current waveform of the MPPT boost converter	86
Figure 3.22	The input capacitor current waveform of the MPPT converter	90
Figure 3.23	The output capacitor current waveform for the MPPT converter	91
Figure 3.24	The flowchart of the MPPT boost converter design	93
Figure 3.25	The simplified P&O MPPT algorithm	94
Figure 4.1	The implementation of the DRM, the RFMPI and the RFMF in MATLAB/Simulink	97
Figure 4.2	The convergence of the PV models at 1000 W/m^2 and 25˚C	99
Figure 4.3	The V_o, I_{ref} and I_o of the conventional DRM at 1000 W/m^2 and 25˚C. a) Default K_i (85.26), b) Retuned K_i (35.00)	101
Figure 4.4	The V_o and I_o of the conventional DRM with the default and overtuned K_i (85.26 and 1.00, respectively) at 25˚C	102

Figure 4.5 The V_o, I_{ref} and I_o of the proposed RFM with, a) the PI controller using the default K_i (85.26) and, b) the fuzzy controller, at 1000 W/m^2 and 25˚C 104

Figure 4.6 The relationship among the error of PVE, PV model and control strategy 105

Figure 4.7 The e_i of the I-V PV model compared to the manufacturer data during different irradiance 107

Figure 4.8 The $e_{\%i(I\text{-}R)}$ during difference G 108

Figure 4.9 a) The steady state response of the PVE mapped to the I-V characteristic curve at 25˚C with the R_o between 5 Ω to 90 Ω. b) The corresponding $e_{\%i(PVE)}$ with respect to PV model 110

Figure 4.10 The steady state response of the PVE mapped to the I-V characteristic curve at 25˚C with R_o lower than 5 Ω and higher than 90 Ω 112

Figure 4.11 The t_s of I_o at various R_o and G. 115

Figure 4.12 The V_o and I_o during the load step change at 1000 W/m^2 and 25˚C 118

Figure 4.13 The V_o and I_o during the irradiance step change at 17 Ω and 25˚C 121

Figure 4.14 The V_o and I_o during the temperature step change at 17 Ω and 1000 W/m^2 122

Figure 4.15 The efficiency of the PVE with respect to the output power at 25°C 123

Figure 4.16 The simulated D_{mppt} using a fixed R_{o_mppt} (135 Ω), tested under the irradiance of 200 W/m^2 and 1000 W/m^2, respectively 125

Figure 4.17 The zoomed-in view of the I_{L_mppt} and the $I_{L\_mppt(ave)}$ waveforms at 1000 W/m^2 127

Figure 4.18 The γ_{IL_mppt} at different irradiance with a fixed R_{o_mppt} of 135 Ω 127

Figure 4.19 The zoomed-in view of the V_{mp} and the $V_{mp(ave)}$ waveforms at 1000 W/m^2 128

Figure 4.20 The γ_{Vmp} using a fixed R_{o_mppt} (135 Ω) under a series of irradiances 129

Figure 4.21 The zoomed-in view of the V_{o_mppt} and the $V_{o\_mppt(ave)}$ waveforms at 1000 W/m^2 130

Figure 4.22 The γ_{Vo_mppt} using a fixed R_{o_mppt} (135 Ω) under a series of irradiances 131

Figure 4.23 The V_o and I_o of the PVE connected to the MPPT converter 132

Figure 4.24 The simulated PVE output voltage and power, mapped to the P V characteristic curves, under 400 W/m^2 and 1000 W/m^2 134

Figure 5.1 The overview of the experimental verification setup 138

Figure 5.2 The circuit representation of the resistor-capacitor-diode (RCD) snubber 139

Figure 5.3 The Analogue to Digital Converter (ADC) Calibration and the Pulse Width Modulation (PWM) activation for dSPACE ds1104 141

Figure 5.4 The block diagram of the sensors and the gate driver connection on dSPACE ds1104 144

Figure 5.5 The experimental results: The V_o and I_o of the conventional DRM at 1000 W/m^2 and 25˚C. a) Default K_i (85.26), b) Retuned K_i (35.00) 152

Figure 5.6 The experimental results of V_o and I_o of the DRM with a) the default K_i and b) the overtuned K_i connected to the MPPT converter at 25˚C 153

Figure 5.7 The experimental results: The V_o and I_o of the proposed RFM with, a) the PI controller using the default K_i (85.26) and, b) the fuzzy controller, at 1000 W/m^2 and 25˚C 154

Figure 5.8 The experimental results: a) The steady state response of the PVE mapped to the I-V characteristic curve at 25˚C with the R_o between 5 Ω to 90 Ω. b) The corresponding $e_{\%i(PVE)}$ with respect to PV model 156

Figure 5.9 The t_s of the control strategy comparison between the simulation and experimental results during start-up at the MPP during the STC 157

Figure 5.10 The experimental results of V_o and I_o with 17 Ω, 1000 W/m^2 and 25˚C. a) DRM. b) RFMPI. c) RFMF 158

Figure 5.11 The t_s of the control strategy comparison between the simulation and experimental results during the load change 160

Figure 5.12 The experimental results of V_o and I_o during the load step change from 10 Ω to 60 Ω at 1000 W/m^2 and 25˚C. a) DRM. b) RFMPI. c) RFMF 161

Figure 5.13 The experimental results of V_o and I_o during the load step change from 10 Ω to 60 Ω at 1000 W/m^2 and 25˚C, (left – overall waveforms, right – the zoomed in view). a) DRM. b) RFMPI. c) RFMF 162

Figure 5.14 The experimental results of V_o and I_o during the irradiance step change from 200 W/m^2 to 1000 W/m^2 at 17 Ω and 25˚C. a) DRM. b) RFMPI. c) RFMF 164

Figure 5.15 The experimental results of V_o and I_o during the irradiance step change from 1000 W/m^2 to 200 W/m^2 at 17 Ω and 25˚C. a) DRM. b) RFMPI. c) RFMF 165

Figure 5.16 The t_s of the control strategy comparison between the simulation and experimental results 166

Figure 5.17 The simulation and experimental PVE's efficiency at the MPP. 167

Figure 5.18 The V_o and I_o of a) the DRM, b) the RFMPI, c) the RFMF when connected to the MPPT converter 168

Figure 5.19 The experimental Power-Voltage output of the PVE when G is 400 W/m^2 and 1000 W/m^2 169

LIST OF ABBREVIATIONS

1D	-	Single Diode
1D1R	-	Single Diode Single Resistance
1D2R	-	Single Diode Double Resistance
2D2R	-	Double Diode Double Resistance
AC	-	Altenating Current
BJT	-	Bipolar Junction Transistor
CCR	-	Constant Current Region
CVR	-	Constant Voltage Region
DAC	-	Digital to Analogue Converter
DC	-	Direct Current
DRM	-	Direct Referencing Method
EMI	-	Electromagnetic Interference
ESR	-	Equivalent Series Resistance
GUI	-	Graphical User Interface
HC	-	Hill Climbing
IC	-	Integrated Circuit
I-R	-	Current-Resistance
I-V	-	Current-Voltage
LED	-	Light Emmitting Diode
LUT	-	Look-Up Table
MOSFET	-	Metal Oxide Semiconductor Field Effect Transistor
MPP	-	Maximum Power Point
MPPT	-	Maximum Power Point Tracking
P&O	-	Perturb and Observe
PI	-	Proportional-Integral
PID	-	Proportional-Integral-Derivative
PV	-	Photovoltaic
PVE	-	Photovoltaic Emulator
P-V	-	Power-Voltage
PWM	-	Pulse Width Modulation
RFM	-	Resistance Feedback Method (General)
RFMPI	-	Resistance Feedback Method using PI Controller
RFMF	-	Resistance Feedback Method using Fuzzy Controller
SMPS	-	Switched-Mode Power Supply
STC	-	Standard Test Condition
ZCS	-	Zero Current Switching
ZVS	-	Zero Voltage Switching

LIST OF SYMBOLS

A	-	System Matrix
A_f	-	Ideality Factor
B	-	Input Matrix
C	-	Capacitance of the Buck Converter
C_{i_mppt}	-	Input Capacitance for MPPT Converter
C_{o_mppt}	-	Output Capacitance for MPPT Converter
D	-	Duty Cycle
D_{max}	-	Maximum Duty Cycle for Buck Converter
D_{min}	-	Minimum Duty Cycle for Buck Converter
$D_{mppt(max)}$	-	Maximum Duty Cycle for MPPT Converter
$D_{mppt(min)}$	-	Minimum Duty Cycle for MPPT Converter
D_{mppt}	-	Duty Cycle for MPPT Converter
D_{step}	-	Duty Cycle Step
E	-	Output Matrix
e	-	Feedback Error
$e_{\%i(I-R)}$	-	Percentage Current Error of I-R PV Model
e_i	-	Absolute Current Error
e_{pve}	-	Photovoltaic Equation Error
F	-	Feedforward Matrix
f_s	-	Switching Frequency
f_{mppt}	-	Switching Frequency for MPPT Converter
f_{pvm}	-	Function of PV Model
f_{pvm}'	-	Derivative Function of PV Model against I_{pv}
G	-	Irradiance
G_b	-	Transfer function for Buck Converter
G_c	-	Transfer function for PI Controller
G_{stc}	-	Irradiance at Standard Test Condition
I_D	-	Diode Current
I_{i_mppt}	-	Input Current for MPPT Converter
I_{mp}	-	Maximum Power Current
$I_{mp\_G(min)}$	-	Maximum Power Current at Minimum Irradiance
I_o	-	Output Current
I_{ph}	-	Photo-Generated Current
I_{pv}	-	Photovoltaic Current
$I_{pv(max)}$	-	Maximum Photovoltaic Current
$I_{pv(min)}$	-	Minimum Photovoltaic Current
I_{pv_model}	-	PV Current obtained from PV Model
I_{pv_module}	-	PV Current obtained from Manufacturer Data
$I_{sc\_G(min)}$	-	Short Circuit Current during Minimum Irradiance
I_{ref}	-	Reference Current
I_s	-	Saturation Current
I_{s1}	-	Saturation Current 1
I_{s2}	-	Saturation Current 2
I_{sc}	-	Short Circuit Current
k	-	Boltzmann Constant

K_d	-	Derivative Gain
K_e	-	Error Gain
K_i	-	Integral Gain
K_{i_mppt}	-	Integral Gain for MPPT Converter
K_p	-	Proportional Gain
K_{p_mppt}	-	Proportional Gain for MPPT Converter
L	-	Inductance of the Buck Converter
$L1$	-	Inductance in Phase One
$L2$	-	Inductance in Phase Two
L_{mppt}	-	Inductance for MPPT Converter
$L_{mppt(4/9)}$	-	Inductance for MPPT Converter with R_{mp} = 4/9 R_{o_mppt} Exist.
$L_{mppt(x4/9)}$	-	Inductance for MPPT Converter with R_{mp} = 4/9 R_{o_mppt} Not Exist.
N_s	-	Number of Cells in Series
OS_{Io}	-	Output Current Overshoot
p-n	-	Positive-Negative
P_{max}	-	Maximum Power
P_{mp}	-	Power at MPP
P_o	-	Output Power
q	-	Electron Charge
r_C	-	Internal Resistance of Capacitor for Buck Converter
r_{Ci_mppt}	-	Internal Resistance of Input Capacitor for MPPT Converter
r_{Co_mppt}	-	Internal Resistance of Output Capacitor for MPPT Converter
$R_{ds(on)}$	-	MOSFET Drain-Source On Resistance
r_L	-	Internal Resistance of Inductor for Buck Converter
r_{L_mppt}	-	Internal Resistance of Inductor for MPPT Converter
$R_{mp(max)}$	-	Maximum Power Resistance at Low Irradiance
$R_{mp(min)}$	-	Maximum Power Resistance at High Irradiance
$R_{mp\_\gamma IL(max)}$	-	Maximum power point resistance with the maximum inductor current ripple factor.
R_o	-	Output Resistance
$R_{o(max)}$	-	Maximum Output Resistance for PVE
$R_{o(min)}$	-	Minimum Output Resistance for PVE
R_{o_mppt}	-	Output Resistance for MPPT Converter
$R_{o\_mppt(max\_G)}$	-	Output Resistance for MPPT Converter at Maximum Irradiance and Maximum Duty Cycle
$R_{o\_mppt(max\_g)}$	-	Output Resistance for MPPT Converter at Minimum Irradiance and Maximum Duty Cycle
$R_{o\_mppt(min\_G)}$	-	Output Resistance for MPPT Converter at Maximum Irradiance and Minimum Duty Cycle
$R_{o\_mppt(min\_g)}$	-	Output Resistance for MPPT Converter at minimum Irradiance and Minimum Duty Cycle
R_{mp}	-	MPP Resistance
$R_{mp(max)}$	-	Maximum MPP Resistance
$R_{mp(min)}$	-	Minimum MPP Resistance
$R_{mp\_\gamma IL(max)}$	-	MPP Resistance with Maximum γ_{IL}
R_p	-	Parellel Resistance
R_{pv}	-	Photovoltaic Resistance

R_s	-	Series Resistance
$State$	-	State
T	-	Temperature
T_{mppt}	-	Switching Period of MPPT Boost Converter
t_{pert}	-	Perturbation Period
t_s	-	Settling Time
T_{stc}	-	Temperature at Standard Test Condition
u	-	Input Matrix
V_f	-	Forward Voltage
V_i	-	Input Voltage
V_{i_mppt}	-	Input Voltage for MPPT Converter
V_{mp}	-	Maximum Power Voltage
$V_{mp\_G(min)}$	-	Maximum Power Voltage at Minimum Irradiance
V_o	-	Output Voltage
V_{oc}	-	Open Circuit Voltage
V_{pv}	-	Photovoltaic Voltage
V_{pv_ref}	-	Reference Photovoltaic Voltage
V_{pv_start}	-	PV Starting Voltage
V_{pv_step}	-	PV Step Voltage
$V_{mp\_G(min)}$	-	Maximum Power Point Voltage at Minimum Irradiance
$V_{oc\_G(min)}$	-	Open Circuit Voltage at Minimum Irradiance
V_T	-	Thermal Voltage
x	-	State-Space Vector
y	-	Output Vector
α	-	Temprature Coefficient of I_{sc}
β	-	Temprature Coefficient of V_{oc}
γ_{IL_mppt}	-	Inductor Current Ripple Factor for MPPT Converter
γ_{Vmp}	-	Maximum Power Point Voltage Ripple Factor for MPPT Converter
γ_{Vo}	-	Output Voltage Ripple Factor for Buck Converter
γ_{Vo_mppt}	-	Output Voltage Ripple Factor for MPPT Converter
ρ_{e_PVE}	-	Accuracy Improvement of PVE
ρ_{ts}	-	Settling Time Improvement
Δi_{L_mppt}	-	Change of MPPT Inductor Current
ΔQ_i	-	Change of Charge in C_{i_mppt}
ΔQ_o	-	Change of Charge in C_{o_mppt}
η	-	Efficiency
ρ_{ts}	-	Settling Time Improvement

LIST OF APPENDICES

APPENDIX	TITLE	PAGE
Appendix A	The Current-Resistance Photovoltaic Model Computed using Binary Search Method	189
Appendix B	State-Space Derivation of the Nonideal Buck Converter	190
Appendix C	Derivation of the Maximum Power Point Tracking Boost Converter for Variable Load	200
Appendix D	Maximum Power Point Tracking Boost Converter MATLAB Script	207
Appendix E	List of Publication	211

CHAPTER 1

INTRODUCTION

1.1 Background of the Study

A recent study shows the potential of the solar based energy generation using the photovoltaic (PV) panel to fulfil the world's energy demand. Solar energy is one of the renewable energies that requires little maintenance, which has low operation cost and pollution free. Up to 2015, there was a 50 GW_p increase annually in the global PV energy production, which totalled up to 227 GW_p of the estimated global capacity of the PV energy [1]. This shows a 22% increase in the global energy production from the PV generation based system. Malaysia has the potential for solar-based energy generation due to its high and steady irradiance throughout the year [2]. There was a 27.1% increase in the PV energy production in Malaysia from 2016 to 2017 [3]. The rise in PV's popularity is due to an increase in awareness of the PV's potential, government programs to promote the use of the renewable energy and the increase in the market competition of the PV.

One of the components in the PV energy generation system is the maximum power point tracking (MPPT). Since the PV module is a nonlinear source, the MPPT ensures the maximum power is extracted from the PV module at any prevailing environmental condition. In the development stage of the MPPT, the PV module is emitted with irradiance from the controllable halogen lamp or the light emitting diode (LED) to test the effectiveness of the MPPT [4]. However, the setup for this test bed is complex and temperature manipulation is not flexible. This method also requires a large area for the actual PV module, the light source and a controllable direct current (DC) or alternating current (AC) source to control the light source. Besides, this method is inefficient since a high power is required by the light source to produce the irradiance for the PV module. These drawbacks can be overcome using an alternative test bed for MPPT testing, which is known as the PV emulator (PVE).

The PVE is a nonlinear power supply which is capable of producing the current-voltage (I-V) characteristic curve of a PV module. The PVE functions as a power source in the experimental stage of the solar energy generating system to allow repeatable testing conditions without sunlight. The PVE offers a convenient control of ambient conditions rather than complex irradiance and temperature control to allow fast and efficient solar energy generation system testing. The PVE available in the market varies from a single panel emulation (approximately 300 W) to a PV array emulation (larger than 300 W). However, this type of PVE is expensive, ranging from (US)$ 6,385 (Elgar ETS60X14C-PVF) to (US)$ 21,000 (Magna Power TSD50050240) [5, 6]. Therefore, much research related to the PVE has been conducted to reduce the overall cost and improve the transient response of the PVE.

In general, there are three components in a PVE system, namely the PV model, the power converter and the control strategy, as shown in Figure 1.1. The PV model is highly responsible for the accuracy, the computational requirement and the adaptability of the PVE, as shown in Figure 1.2. The PVE require real-time calculation of the PV model to operate properly. The delays in the computation of the PV model results in incorrect output for the PVE. Therefore, the PV model used in the PVE application needs to be simple enough without compromising the accuracy of the I-V characteristic produced [7]. This accuracy and simplicity depend on the type and implementation method of the PV model. The types of PV models include the Interpolation Model and the Electrical Circuit Model. While the implementation methods of the PV model includes the PV model simplification [8-12], Look-Up Table (LUT) [13-18], Piecewise Linear Method [19-22], and Neural Network [9, 23]. The PV model implementation method affects the adaptability of the PVE since some of the methods require offline adjustment of the PV model parameters.

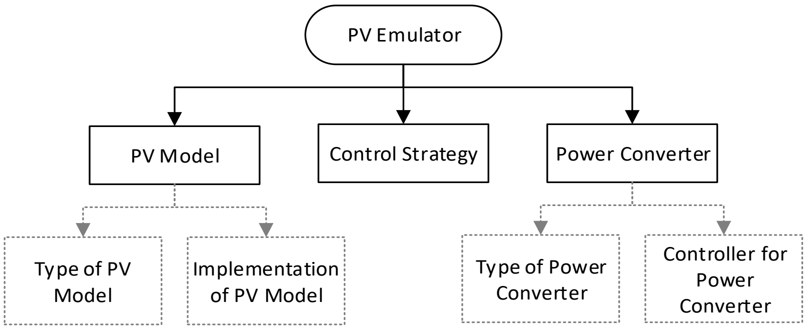

Figure 1.1: The three components of the PVE system.

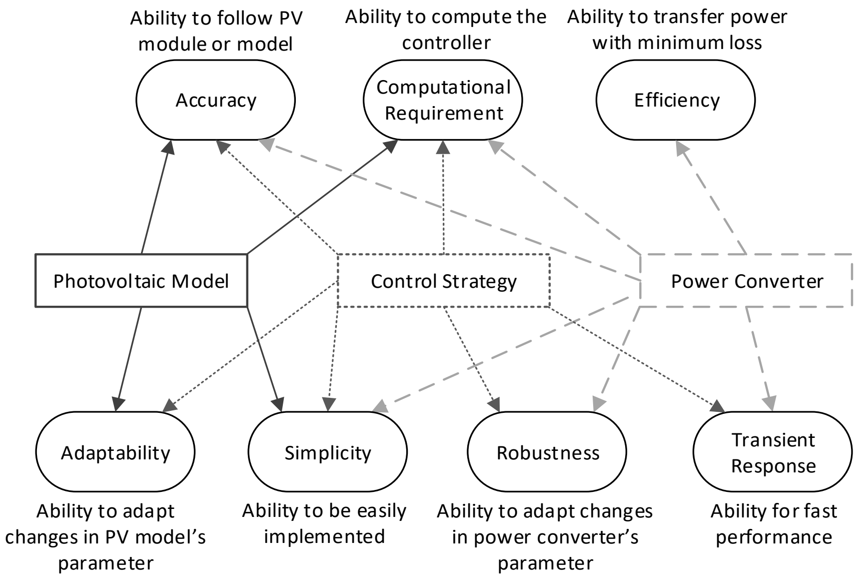

Figure 1.2: The influence of the three components in the PVE system toward the performance of the PVE.

The power converter is also a part of the PVE system. It affects the robustness, transient response, the efficiency and the computational requirement of the PVE. The actual PV panel response approximately tenth of microseconds [24]. Therefore, the PVE is aimed to have a fast response time similar to an actual PV panel. The performance depends on the type and controller of the power converter. The switched-mode power supply (SMPS) is commonly used in the PVE and is highly efficient [18, 25-28]. The linear regulator is useful if the output ripple for the PVE needs to be removed [29-32]. The design of the PVE using the programmable power supply is simple since the closed-loop system for the power converter is already included in the system [33-35]. While the commonly used controller for the power converter is the proportional-integral (PI) or proportional-integral-derivative (PID) controllers [24, 28, 36, 37]. There is also the fuzzy PI or PID controllers [38, 39] and the sliding mode controller [40, 41].

The control strategy of the PVE is the method used to obtain the operating point based on the given load, irradiance and temperature. It combines the PV model and power converter to become PVE. The control strategy affects the various performance of the PVE. A good control strategy features accurate output voltage and output current similar to the PV model, easily implemented, robustness, fast transient response, high adaptability in emulating various PV model and low processing burden. There are several control strategies used in PVE implementation. The direct referencing method (DRM) is commonly used in the PVE due to its simplicity [9, 11, 39, 42-44]. The hybrid-mode control method [29, 33, 45] and the resistance comparison method [26, 28, 46] produce a stable output for the PVE at any load condition. The hill climbing (HC) method for the PVE is easily designed since a compensator is not required [47, 48]. The analogue based method does not have a computational delay and the partial shading condition is easily emulated [44, 49-52].

1.2 Problem Statement

The commonly used control strategy in PVE is the DRM due to its simplicity in implementation. The PVE is formed by connecting the PV model directly to the input reference of the closed-loop controller in the power converter. The operating point of the PVE using the DRM is determined by the PI controller and the buck converter. This is not a robust control strategy because any changes in the PI controller gains and the buck converter output may result in oscillation or instability in the PVE output voltage and current. Besides, the design of the PI controller is affected by the DRM and the process of tuning the PI controller gains becomes complicated. To avoid these problems, the hybrid-mode control method and the resistance comparison method is introduced. The hybrid-mode control method combines two types of DRMs, namely the voltage-mode and current-mode control. The voltage-mode control DRM produces a non-oscillate and stable PVE output in I-V characteristic curve over the constant voltage region (CVR); yet the PVE output oscillates or becomes unstable when it moves over the constant current region (CCR), shown in Figure 1.3. Contrary, the current-mode control DRM produces a non-oscillate and stable PVE output in the CCR, but oscillates or becomes unstable in the CVR. Therefore, hybridise the operation of the PVE in the voltage-mode control DRM over the CVR and the current-mode control DRM over the CCR, non-oscillate and stable output of PVE can be achieved. Besides, the dependency of the hybrid-mode control method on the power converter and its controller is minimized, which ease the tuning of the PI controller. Nevertheless, the implementation becomes complicated since two different PV models and PI controllers are needed. An additional algorithm to switch between two DRMs is also needed in the control strategy. On the other hand, the resistance comparison method is robust since it computes the PVE operating point using the iterative method instead of relies on the power converter and its controller. This control strategy computes various data points in the I-V characteristic curve of the PV model and compares it with the output resistance before reaching the true operating point. Therefore, a high computational power is needed to avoid delays in producing the PVE operating points. Delay in computational results in inaccurate output voltage and current of the PVE. Acknowledged the benefits and drawbacks of the control strategies, an improved control strategy features a robust characteristic, simple implementation and low computational power has been proposed.

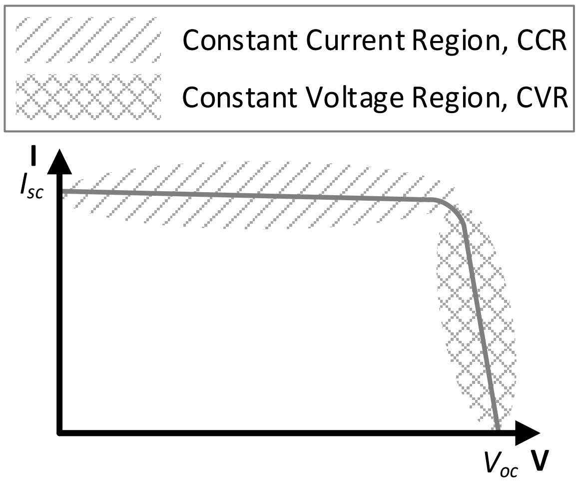

Figure 1.3: The area of the constant current and voltage regions in the PV I-V characteristic curve.

The PI controller for the closed-loop buck converter is designed specifically for a load condition. Even though this PI controller is able to operate under other load conditions, the performance of the buck converter decreases significantly. As the load increases, the settling time for the output voltage and current of the closed-loop buck converter increases. Conversely, the PI controller used in the PVE with the DRM produces a low settling time for the PVE output voltage and current when the output resistance is high. The fast performance of the DRM at high output resistance is due to the high input reference during the transient response that causing the duty cycle to change quickly. Still, the PVE with the DRM performs slowly when output resistance is low. Consequently, the characteristics of the conventional PI controller for the closed-loop buck converter during low output resistance and the DRM during high output resistance are desired. Hence, this combination produces fast output voltage and current response for the buck converter at various load condition. These characteristics can be applied to the fuzzy controller in order to improve the performance of the PVE.

1.3 Research Objectives

The objectives of the research are:

1. To design a control strategy for the PVE features robust characteristic, simple implementation and low computational power.

2. To improve the transient performance of the PVE at various load conditions using the fuzzy controller.

3. To validate the proposed PVE system experimentally and benchmarked with the DRM.

1.4 Research Methodology

Firstly, the literature review on the PVE is conducted. In the review, the control strategy, PV model and power converter used in the PVE is analysed. The advantages and disadvantages of the various components in the PVE are investigated based on the simulations and experiments conducted on the PVE. The problems faced by the conventional PVE is studied and the new controller for the PVE is suggested to overcome these problems.

The new controller for the PVE is simulated using MATLAB/Simulink. A PV module is chosen during the emulation process. The performances of the PVE are analysed using the resistive load and the maximum power point tracking (MPPT) boost converter. The results from the new controller is compared with the conventional controller.

Lastly, the simulation results are experimentally validated, which the controllers for the PVEs are implemented in dSPACE ds1104 rapid prototyping. The experimental results is observed using an oscilloscope and dSPACE ControlDesk software package.

1.5 Research Contribution

The thesis presents the proposed work on PVE research with contributions as follow:

1. To proposes a control strategy called the resistance feedback method (RFM), which requires only a single iteration of the PV model to produce an operating point. It is highly accurate, easily implemented, robust against various changes in the parameters of the power converter and its controller, adapts to various PV module, and produces fast output voltage and current response.

2. To proposes a modified current-resistance (I-R) PV model which the input to the PV model is the resistance. It is computed using the binary search method. This model allows the change of irradiance and temperature during operation, which is highly accurate and easily implemented. This PV model is suitable for the RFM.

3. To proposes a fuzzy controller for the buck converter called the fuzzy error compensator, which is capable of maintaining fast response at various load conditions. The fuzzy error compensator is integrated into the RFM to further improve the performance of the PVE.

4. To develops a procedure to design the boost converter specifically for the MPPT application. This allows simple calculations of the passive components in the MPPT boost converter.

The first three contributions improve all three components of the PVE system as shown in Figure 1.4. While the last contribution improves the results obtained when the PVE is connected to the MPPT converter.

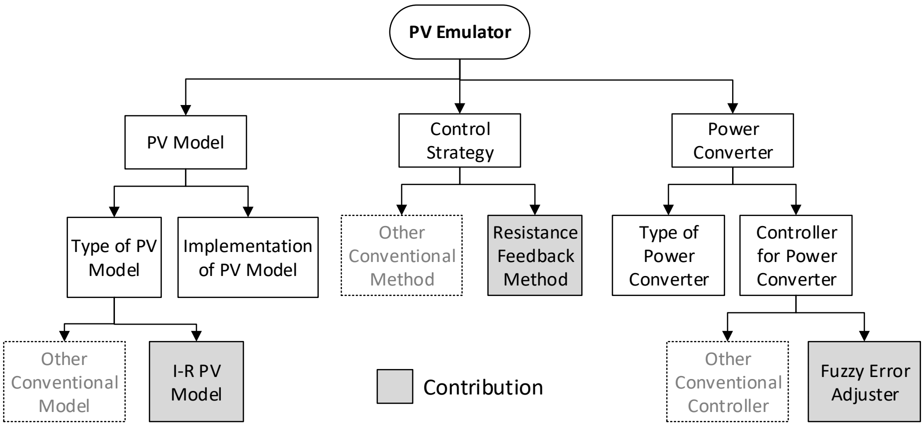

Figure 1.4: The contribution categories based on the components of the PVE system.

1.6 Scope of the Study

The simulation of the PVE is done using the MATLAB/Simulink software package. The improvement of the PVE focused on the control strategy, PV model and the controller for the power converter. There is no modification on the type of power converter used in the PVE. The PVE is able to emulate the PV module with the open circuit voltage of 44.4 V, the short circuit current of 2.32 A and the maximum power of 75.7 W_p. The single diode model is used as the PV model. The PVE requires real-time calculation of the PV model. Therefore, the PV model used for PVE application needs to compromise between the complexity and the accuracy.

The buck converter is chosen as the power converter for the PVE since it is efficient, able to operate at various condition and easily controlled. The load for the PVE is a resistive load and the MPPT boost converter with the perturb and observe (P&O) method. The performance of the proposed controller is benchmarked with the conventional DRM. The controller for the PVE is implemented using the dSPACE ds1104 rapid prototyping board and it is monitored using the dSPACE ControlDesk software package.

In this thesis, the partial shading is not considered in the PVE since the real-time calculation of the PV model burdens the digital hardware platform. The load of the PVE ranges from 5 Ω to 90 Ω. The short and open circuit tests are not conducted due to the limitation of the buck converter. The PVE and MPPT boost converter is designed to operate with the irradiance between 200 W/m^2 to 1000 W/m^2 and temperature between 0°C to 75°C. During this condition, the PVE and MPPT boost converter operates in the continuous current-mode. The operation outside the irradiance and temperature ranges may result in a large voltage ripple, inaccurate emulation and damages to the components. The standard test condition (STC), which is 1000 W/m^2 and 25°C, is used to analyse the performance of the PVEs. Nonetheless, the designed PVE and MPPT boost converter capable of operating within the real-world irradiance and temperature condition.

1.7 Thesis Organization

The thesis is organised as follows:

Chapter 2 reviews the various types and implementation of the PV model, the types of power converter and its controller, and several types of the control strategy. The benefits and drawbacks of each component are also discussed.

Chapter 3 discusses the methodology of the conventional single diode PV model used in the PVE. The design of the buck converter and the derivation of the transfer function are reported in this chapter. There are two controllers for the buck converter, namely the conventional PI controller and the proposed fuzzy error compensator. The procedure for developing the conventional DRM, the proposed RFM with PI controller (RFMPI) and the proposed RFM with the fuzzy controller (RFMF) are elaborated in this chapter. The proposed design procedure of the MPPT boost converter is also derived.

Chapter 4 discusses the simulation results of the conventional DRM, the proposed RFMPI and the proposed RFMF. This chapter covers the convergence of one data point in the I-V characteristic curve using the conventional and the proposed PV model. In addition, the robustness, accuracy and transient response of the control strategy are detailed. The performance of the PVE when it is connected to the MPPT converter is also analysed. The derived equations of the MPPT boost converter are validated using simulations.

Chapter 5 discusses the experimental results of the conventional DRM, the proposed RFMPI and the proposed RFMF. The procedure for developing the experimental set-up is discussed in this chapter. The experimental results are compared with the simulation results in order to validate the proposed method.

Chapter 6 draws the conclusion of the thesis and provides possible directions for further research.

REFERENCES

[1] REN21, "Renewables 2016 Global Status Report (GSR)," 2016.

[2] A. Belhamadia, M. Mansor, and M. A. Younis, "Assessment of wind and solar energy potentials in Malaysia," in *Clean Energy and Technology (CEAT), 2013 IEEE Conference on*, 2013, pp. 152-157.

[3] S. Malaysia. (2018). *Sustainable Energy Development Authority (SEDA) Malaysia: Renewable Energy Generation*. Available: http://www.seda.gov.my/

[4] S. Armstrong, C. K. Lee, and W. G. Hurley, "Investigation of the harmonic response of a photovoltaic system with a solar emulator," in *Power Electronics and Applications, 2005 European Conference on*, 2005, pp. 8 pp.-P.8.

[5] *Ametek Programmable Power*. Available: http://www.programmablepower.com/

[6] *Magma Power*. Available: http://www.magna-power.com/

[7] E. Lattanzi, M. Dromedari, V. Freschi, and A. Bogliolo, "Tuning the complexity of photovoltaic array models to meet real-time constraints of embedded energy emulators," *Energies*, vol. 10, 2017.

[8] M. C. Di Piazza, M. Pucci, A. Ragusa, and G. Vitale, "A grid-connected system based on a real time PV emulator: Design and experimental set-up," in *IECON 2010 - 36th Annual Conference on IEEE Industrial Electronics Society*, 2010, pp. 3237-3243.

[9] M. C. Di Piazza, M. Pucci, A. Ragusa, and G. Vitale, "Analytical Versus Neural Real-Time Simulation of a Photovoltaic Generator Based on a DC-DC Converter," *IEEE Transactions on Industry Applications*, vol. 46, pp. 2501-2510, 2010.

[10] D. Ickilli, H. Can, and K. S. Parlak, "Development of a FPGA-based photovoltaic panel emulator based on a DC/DC converter," in *Photovoltaic Specialists Conference (PVSC), 2012 38th IEEE*, 2012, pp. 001417-001421.

[11] D. Abbes, A. Martinez, G. Champenois, and B. Robyns, "Real time supervision for a hybrid renewable power system emulator," *Simulation Modelling Practice and Theory*, vol. 42, pp. 53-72, 3// 2014.

[12] Y. Erkaya, P. Moses, I. Flory, and S. Marsillac, "Steady-state performance optimization of a 500 kHz photovoltaic module emulator," in *2016 IEEE 43rd Photovoltaic Specialists Conference (PVSC)*, 2016, pp. 3205-3208.

[13] M. T. Iqball, M. Tariq, M. K. Ahmad, and M. S. B. Arit, "Modeling, analysis and control of buck converter and Z-source converter for photo voltaic emulator," in *2016 IEEE 1st International Conference on Power Electronics, Intelligent Control and Energy Systems (ICPEICES)*, 2016, pp. 1-6.

[14] Z. Weichao and J. W. Kimball, "DC-DC converter based photovoltaic simulator with a double current mode controller," in *2016 IEEE Power and Energy Conference at Illinois (PECI)*, 2016, pp. 1-6.

[15] S. Gadelovits, M. Sitbon, and A. Kuperman, "Rapid Prototyping of a Low-Cost Solar Array Simulator Using an Off-the-Shelf DC Power Supply," *IEEE Transactions on Power Electronics*, vol. 29, pp. 5278-5284, 2014.

[16] E. Koutroulis, K. Kalaitzakis, and V. Tzitzilonis, "Development of an FPGA-based system for real-time simulation of photovoltaic modules," *Microelectronics Journal,* vol. 40, pp. 1094-1102, 2009.
[17] L. M. Barrera, R. A. Osorio, and C. L. Trujillo, "Design and implementation of electronic equipment that emulates photovoltaic panels," in *Photovoltaic Specialist Conference (PVSC), 2015 IEEE 42nd*, 2015, pp. 1-5.
[18] González-Medina, Raúl Patrao, Iván Garcerá, Gabriel Figueres, and Emilio, "A low-cost photovoltaic emulator for static and dynamic evaluation of photovoltaic power converters and facilities," *Progress in Photovoltaics: Research and Applications,* vol. 22, pp. 227-241, 2012.
[19] G. Martin-Segura, J. Lopez-Mestre, M. Teixido-Casas, and A. Sudria-Andreu, "Development of a photovoltaic array emulator system based on a full-bridge structure," in *Electrical Power Quality and Utilisation, 2007. EPQU 2007. 9th International Conference on*, 2007, pp. 1-6.
[20] H. Abidi, A. B. Ben Abdelghani, and D. Montesinos-Miracle, "MPPT algorithm and photovoltaic array emulator using DC/DC converters," in *Electrotechnical Conference (MELECON), 2012 16th IEEE Mediterranean*, 2012, pp. 567-572.
[21] Z. Ziming, Z. Jianwen, S. Haimeng, W. Gang, H. Xiwen, and Z. Shi, "Research on Photovolta Array Emulator System Based on A Novel Zero-Voltage Zero-Current Switching Converterer," in *Power and Energy Engineering Conference (APPEEC), 2010 Asia-Pacific*, 2010, pp. 1-4.
[22] D. D. C. Lu and Q. N. Nguyen, "A photovoltaic panel emulator using a buck-boost DC/DC converter and a low cost micro-controller," *Solar Energy,* vol. 86, pp. 1477-1484, 5// 2012.
[23] F. Gomez-Castaneda, G. M. Tornez-Xavier, L. M. Flores-Nava, O. Arellano-Cardenas, J. A. Moreno-Cadenas, and Ieee, "Photovoltaic panel emulator in FPGA technology using ANFIS approach," in *2014 11th International Conference on Electrical Engineering, Computing Science and Automatic Control (Cce)*, 2014, p. 6.
[24] K. Nguyen-Duy, A. Knott, and M. A. E. Andersen, "High Dynamic Performance Nonlinear Source Emulator," *IEEE Transactions on Power Electronics,* vol. 31, pp. 2562-2574, Mar 2016.
[25] A. Vijayakumari, A. T. Devarajan, and N. Devarajan, "Design and development of a model-based hardware simulator for photovoltaic array," *International Journal of Electrical Power & Energy Systems,* vol. 43, pp. 40-46, 12// 2012.
[26] A. V. Rana and H. H. Patel, "Current controlled buck converter based photovoltaic emulator," *Journal of Industrial and Intelligent Information,* vol. 1, 2013.
[27] C.-C. Chen, H.-C. Chang, C.-C. Kuo, and C.-C. Lin, "Programmable energy source emulator for photovoltaic panels considering partial shadow effect," *Energy,* vol. 54, pp. 174-183, 6/1/ 2013.
[28] C. H. Balakishan and N. Sandeep, "Development of a Microcontroller Based PV Emulator with Current Controlled DC-DC Buck Converter " *International Journal of Renewable Energy Research,* vol. 4, p. 1, 22 November 2014.
[29] Y. Kim, W. Lee, M. Pedram, and N. Chang, "Dual-mode power regulator for photovoltaic module emulation," *Applied energy,* vol. 101, pp. 730-739, 2013.

[30] D. M. K. Schofield, M. P. Foster, and D. A. Stone, "Low-cost solar emulator for evaluation of maximum power point tracking methods," *Electronics Letters,* vol. 47, pp. 208-209, 2011.
[31] K.-H. Tang, K.-H. Chao, Y.-W. Chao, and J.-P. Chen, "Design and implementation of a simulator for photovoltaic modules," *International Journal of Photoenergy,* vol. 2012, 2012.
[32] S. Jin and D. Zhang, "A simple control method of open-circuit voltage for the FPGA-based solar array simulator," in *Power and Renewable Energy (ICPRE), IEEE International Conference on Power and*, 2016, pp. 209-216.
[33] T. D. Mai, S. De Breucker, K. Baert, and J. Driesen, "Reconfigurable emulator for photovoltaic modules under static partial shading conditions," *Solar Energy,* vol. 141, pp. 256-265, 1 January 2017.
[34] V. Rajguru, K. Gadge, S. Karyakarte, S. Kawathekar, and V. Menon, "Design and implementation of a prototype DC photovoltaic power system simulator with Maximum Power Point Tracking system," in *2016 IEEE 1st International Conference on Power Electronics, Intelligent Control and Energy Systems (ICPEICES)*, 2016, pp. 1-5.
[35] A. Xenophontos, J. Rarey, A. Trombetta, and A. M. Bazzi, "A flexible low-cost photovoltaic solar panel emulation platform," in *Power and Energy Conference at Illinois (PECI)*, 2014, pp. 1-6.
[36] L. P. Sampaio and S. A. O. d. Silva, "Graphic computational platform integrated with an electronic emulator dedicated to photovoltaic systems teaching," *IET Power Electronics,* vol. 10, pp. 1982-1992, 2017.
[37] U. K. Shinde, S. G. Kadwane, R. K. Keshri, and S. Gawande, "Dual Mode Controller-Based Solar Photovoltaic Simulator for True PV Characteristics," *Canadian Journal of Electrical and Computer Engineering,* vol. 40, pp. 237-245, 2017.
[38] W. Shao, Z. Q. Meng, H. A. Zhou, and K. Zhang, "A photovoltaic array simulator based on current feedback fuzzy PID control," *Journal of Intelligent and Fuzzy Systems,* vol. 29, pp. 2555-2564, 2015.
[39] J. Zhang, S. Wang, Z. Wang, and L. Tian, "Design and realization of a digital PV simulator with a push-pull forward circuit," *Journal of Power Electronics,* vol. 14, pp. 444-457, 2014.
[40] U. K. Shinde, S. G. Kadwane, S. P. Gawande, and R. Keshri, "Solar PV emulator for realizing PV characteristics under rapidly varying environmental conditions," in *2016 IEEE International Conference on Power Electronics, Drives and Energy Systems (PEDES)*, 2016, pp. 1-5.
[41] A. Cordeiro, D. Foito, V. Fern, and P. o, "A PV panel simulator based on a two quadrant DC/DC power converter with a sliding mode controller," in *2015 International Conference on Renewable Energy Research and Applications (ICRERA),* 2015, pp. 928-932.
[42] C. Roncero-Clemente, E. Romero-Cadaval, V. Minambres, M. Guerrero-Martinez, and J. Gallardo-Lozano, "PV Array Emulator for Testing Commercial PV Inverters," *Elektronika ir Elektrotechnika,* vol. 19, pp. 71-75, 2013.
[43] A. Koran, T. LaBella, and J. S. Lai, "High Efficiency Photovoltaic Source Simulator with Fast Response Time for Solar Power Conditioning Systems Evaluation," *IEEE Transactions on Power Electronics,* vol. 29, pp. 1285-1297, 2014.

[44] A. Koran, K. Sano, K. Rae-Young, and L. Jih-Sheng, "Design of a Photovoltaic Simulator With a Novel Reference Signal Generator and Two-Stage LC Output Filter," *IEEE Transactions on Power Electronics,* vol. 25, pp. 1331-1338, 2010.

[45] L. Yuan, L. Taewon, F. Z. Peng, and L. Dichen, "A Hybrid Control Strategy for Photovoltaic Simulator," in *Applied Power Electronics Conference and Exposition, 2009. APEC 2009. Twenty-Fourth Annual IEEE*, 2009, pp. 899-903.

[46] Z. Qingrong, S. Pinggang, and C. Liuchen, "A photovoltaic simulator based on DC chopper," in *Electrical and Computer Engineering, 2002. IEEE CCECE 2002. Canadian Conference on*, 2002, pp. 257-261 vol.1.

[47] Y. Erkaya, P. Moses, I. Flory, S. Marsillac, and Ieee, "Development of a Solar Photovoltaic Module Emulator," in *2015 Ieee 42nd Photovoltaic Specialist Conference*, New York, 2015.

[48] J. Gonzalez-Llorente, A. Rambal-Vecino, L. A. Garcia-Rodriguez, J. C. Balda, and E. I. Ortiz-Rivera, "Simple and efficient low power photovoltaic emulator for evaluation of power conditioning systems," in *2016 IEEE Applied Power Electronics Conference and Exposition (APEC)*, 2016, pp. 3712-3716.

[49] O. M. Midtgard, "A simple photovoltaic simulator for testing of power electronics," in *Power Electronics and Applications, 2007 European Conference on*, 2007, pp. 1-10.

[50] H. Nagayoshi, "I–V curve simulation by multi-module simulator using I–V magnifier circuit," *Solar Energy Materials and Solar Cells,* vol. 82, pp. 159-167, 5/1/ 2004.

[51] A. Zegaoui, M. Aillerie, P. Petit, and J.-P. Charles, "Universal Transistor-based hardware SIMulator for real time simulation of photovoltaic generators," *Solar Energy,* vol. 134, pp. 193-201, 9// 2016.

[52] Z. Zhou, P. M. Holland, and P. Igic, "MPPT algorithm test on a photovoltaic emulating system constructed by a DC power supply and an indoor solar panel," *Energy Conversion and Management,* vol. 85, pp. 460-469, 9// 2014.

[53] S. K. Garai, "A Photovoltaic Cell Emulator," Master of Technology in Instrumentation & Electronics Engineering Department of Instrumentation and Electronics Engineering, Jadavpur University, Kolkata, West Bengal, India, 2013.

[54] K. Khouzam and K. Hoffman, "Real-time simulation of photovoltaic modules," *Solar Energy,* vol. 56, pp. 521-526, 1996.

[55] J.-P. Lee, B.-D. Min, T.-J. Kim, J.-H. Kim, M.-H. Ryu, J.-W. Baek, *et al.*, "Development of a photovoltaic simulator with novel simulation method of photovoltaic characteristics," in *Telecommunications Energy Conference, 2009. INTELEC 2009. 31st International*, 2009, pp. 1-5.

[56] M. C. D. Piazza and G. Vitale, "Photovoltaic Sources: Modelling and Emulation," ed: Springer Science & Business Media, 2012.

[57] J. Agrawal and M. Aware, "Photovoltaic system emulator," in *Power Electronics, Drives and Energy Systems (PEDES), 2012 IEEE International Conference on*, 2012, pp. 1-6.

[58] A. M. Koran, "Photovoltaic Source Simulators for Solar Power Conditioning Systems: Design Optimization, Modeling, and Control " Doctor of Philosophy Virginia Polytechnic Institute and State University, Blacksburg, Virginia 2013.

[59] J. Cubas, S. Pindado, and M. Victoria, "On the analytical approach for modeling photovoltaic systems behavior," *Journal of Power Sources,* vol. 247, pp. 467-474, 2014.

[60] M. De Blas, J. Torres, E. Prieto, and A. Garcıa, "Selecting a suitable model for characterizing photovoltaic devices," *Renewable energy,* vol. 25, pp. 371-380, 2002.

[61] P. Hyeonah and K. Hyosung, "PV cell modeling on single-diode equivalent circuit," in *Industrial Electronics Society, IECON 2013 - 39th Annual Conference of the IEEE*, 2013, pp. 1845-1849.

[62] X. Lingyun, S. Lefei, H. Wei, and J. Cong, "Solar cells parameter extraction using a hybrid genetic algorithm," in *Measuring Technology and Mechatronics Automation (ICMTMA), 2011 Third International Conference on*, 2011, pp. 306-309.

[63] J. H. Agrawal and M. V. Aware, "Photovoltaic simulator developed in LabVIEW for evalution of MPPT techniques," in *2016 International Conference on Electrical, Electronics, and Optimization Techniques (ICEEOT)*, 2016, pp. 1142-1147.

[64] W. De Soto, S. Klein, and W. Beckman, "Improvement and validation of a model for photovoltaic array performance," *Solar energy,* vol. 80, pp. 78-88, 2006.

[65] K. Ishaque, Z. Salam, and Syafaruddin, "A comprehensive MATLAB Simulink PV system simulator with partial shading capability based on two-diode model," *Solar Energy,* vol. 85, pp. 2217-2227, 9// 2011.

[66] A. C. Atoche, J. V. Castillo, J. Ortegón-Aguilar, R. Carrasco-Alvarez, J. S. Gío, and A. Colli-Menchi, "A high-accuracy photovoltaic emulator system using ARM processors," *Solar Energy,* vol. 120, pp. 389-398, 2015.

[67] F. Attivissimo, A. D. Nisio, M. Savino, and M. Spadavecchia, "Uncertainty analysis in photovoltaic cell parameter estimation," *Instrumentation and Measurement, IEEE Transactions on,* vol. 61, pp. 1334-1342, 2012.

[68] N. Belhaouas, M. A. Cheikh, A. Malek, and C. Larbes, "Matlab-Simulink of photovoltaic system based on a two-diode model simulator with shaded solar cells," *Revue RER,* vol. 16, pp. 65-73, 2013.

[69] S. Chowdhury, S. Chowdhury, G. Taylor, and Y. Song, "Mathematical modelling and performance evaluation of a stand-alone polycrystalline PV plant with MPPT facility," in *Power and Energy Society General Meeting-Conversion and Delivery of Electrical Energy in the 21st Century, 2008 IEEE*, 2008, pp. 1-7.

[70] M. C. Di Piazza, M. Luna, A. Ragusa, and G. Vitale, "A dynamic model of a photovoltaic generator based on experimental data," in *Renew Energy Power Qual J. ISSN*, 2010.

[71] J. Gow and C. Manning, "Development of a photovoltaic array model for use in power-electronics simulation studies," in *Electric Power Applications, IEE Proceedings-*, 1999, pp. 193-200.

[72] J. A. Jervase, H. Bourdoucen, and A. Al-Lawati, "Solar cell parameter extraction using genetic algorithms," *Measurement Science and Technology,* vol. 12, p. 1922, 2001.

[73] L. Sandrolini, M. Artioli, and U. Reggiani, "Numerical method for the extraction of photovoltaic module double-diode model parameters through cluster analysis," *Applied Energy,* vol. 87, pp. 442-451, 2010.

[74] S. M. Azharuddin, M. Vysakh, H. V. Thakur, B. Nishant, T. S. Babu, K. Muralidhar, *et al.*, "A Near Accurate Solar PV Emulator Using dSPACE Controller for Real-time Control," in *Energy Procedia*, 2014, pp. 2640-2648.

[75] M. Balato, L. Costanzo, D. Gallo, C. Landi, M. Luiso, and M. Vitelli, "Design and implementation of a dynamic FPAA based photovoltaic emulator," *Solar Energy*, vol. 123, pp. 102-115, 1// 2016.

[76] F. Barra, M. Balato, L. Costanzo, D. Gallo, C. Landi, M. Luiso, *et al.*, "Dynamic and Reconfigurable Photovoltaic Emulator Based on FPAA," 2014.

[77] D. Dolan, J. Durago, J. Crowfoot, and Taufik, "Simulation of a photovoltaic emulator," in *North American Power Symposium (NAPS), 2010*, 2010, pp. 1-7.

[78] J. G. Durago, "Photovoltaic Emulator Adaptable To Irradiance, Temperature and Panel-Specific I-V Curves," Master of Science in Electrical Engineering, Electrical Engineering, California Polytechnic State University, San Luis Obispo, California, United States, 2011.

[79] W. Lee, Y. Kim, Y. Wang, N. Chang, M. Pedram, and S. Han, "Versatile high-fidelity photovoltaic module emulation system," in *Proceedings of the 17th IEEE/ACM international symposium on Low-power electronics and design*, 2011, pp. 91-96.

[80] P. G. Bernal, "Study and Development of a Photovoltaic Panel Simulator," Master in Electrical and Computers Engineering University of Porto, 2012.

[81] A. F. Ebrahim, S. M. W. Ahmed, S. E. Elmasry, and O. A. Mohammed, "Implementation of a PV emulator using programmable DC power supply," in *SoutheastCon 2015*, 2015, pp. 1-7.

[82] J. Ollila, "A medium power PV-array simulator with a robust control strategy," in *Control Applications, 1995., Proceedings of the 4th IEEE Conference on*, 1995, pp. 40-45.

[83] T. P. V. Preethishri, K. S. Kumar, and P. Sivakumar, "Embedded emulator of photovoltaic array and wind driven induction generator by using digital signal controller (tms320f28335)," in *Power Electronics (IICPE), 2010 India International Conference on*, 2011, p. 1.

[84] R. G. Wandhare and V. Agarwal, "A low cost, light weight and accurate photovoltaic emulator," in *Photovoltaic Specialists Conference (PVSC), 2011 37th IEEE*, 2011, pp. 001887-001892.

[85] K. Ding, X. Bian, H. Liu, and T. Peng, "A MATLAB-simulink-based PV module model and its application under conditions of nonuniform irradiance," *Energy Conversion, IEEE Transactions on*, vol. 27, pp. 864-872, 2012.

[86] K. Leban and E. Ritchie, "Selecting the accurate solar panel simulation model," in *Nordic Workshop on Power and Industrial Electronics (NORPIE/2008), June 9-11, 2008, Espoo, Finland*, 2008.

[87] G. Walker, "Evaluating MPPT converter topologies using a MATLAB PV model," *Journal of Electrical & Electronics Engineering, Australia*, vol. 21, pp. 49-56, 2001.

[88] Y. Yusof, S. H. Sayuti, M. Abdul Latif, and M. Z. C. Wanik, "Modeling and simulation of maximum power point tracker for photovoltaic system," in *Power and Energy Conference, 2004. PECon 2004. Proceedings. National*, 2004, pp. 88-93.

[89] B. D. Patel and A. Rana, "A pole-placement approach for buck converter based PV array Emulator," in *2016 IEEE 1st International Conference on Power*

Electronics, Intelligent Control and Energy Systems (ICPEICES), 2016, pp. 1-5.
[90] P. J. Binduhewa and M. Barnes, "Photovoltaic emulator," in *Industrial and Information Systems (ICIIS), 2013 8th IEEE International Conference on*, 2013, pp. 519-524.
[91] N. A. Kamarzaman and C. W. Tan, "A comprehensive review of maximum power point tracking algorithms for photovoltaic systems," *Renewable and Sustainable Energy Reviews*, vol. 37, pp. 585-598, September 2014.
[92] V. J. Chin, Z. Salam, and K. Ishaque, "Cell modelling and model parameters estimation techniques for photovoltaic simulator application: A review," *Applied Energy*, vol. 154, pp. 500-519, 15 September 2015.
[93] Y. T. Seo, J. Y. Park, and S. J. Choi, "A rapid I-V curve generation for PV model-based solar array simulators," in *ECCE 2016 - IEEE Energy Conversion Congress and Exposition, Proceedings*, 2016.
[94] J. Yuncong, J. A. A. Qahouq, and I. Batarseh, "Improved solar PV cell Matlab simulation model and comparison," in *Circuits and Systems (ISCAS), Proceedings of 2010 IEEE International Symposium on*, 2010, pp. 2770-2773.
[95] H. Bellia, R. Youcef, and M. Fatima, "A detailed modeling of photovoltaic module using MATLAB," *NRIAG Journal of Astronomy and Geophysics*, vol. 3, pp. 53-61, 6// 2014.
[96] H. Can, D. Ickilli, K. S. Parlak, and Ieee, "A New Numerical Solution Approach for the Real-Time Modeling of Photovoltaic Panels," in *2012 Asia-Pacific Power and Energy Engineering Conference*, New York, 2012.
[97] D. S. L. Dolan, J. Durago, and Taufik, "Development of a photovoltaic panel emulator using Labview," in *Photovoltaic Specialists Conference (PVSC), 2011 37th IEEE*, 2011, pp. 001795-001800.
[98] J. Zhao and J. W. Kimball, "A digitally implemented photovoltaic simulator with a double current mode controller," in *2012 Twenty-Seventh Annual IEEE Applied Power Electronics Conference and Exposition (APEC)*, 2012, pp. 53-58.
[99] A. M. Koran, "Photovoltaic Source Simulators for Solar Power Conditioning Systems: Design Optimization, Modeling, and Control " Doctor of Philosophy, Faculty of the Virginia Polytechnic Institute and State University, Virginia Polytechnic Institute and State University, 2013.
[100] D. S. H. Chan and J. C. H. Phang, "Analytical methods for the extraction of solar-cell single- and double-diode model parameters from I-V characteristics," *Electron Devices, IEEE Transactions on*, vol. 34, pp. 286-293, 1987.
[101] J. Chavarría, D. Biel, F. Guinjoan, A. Poveda, F. Masana, and E. Alarcón, "FPGA-based design of a step-up photovoltaic array emulator for the test of PV grid-connected inverters," in *Industrial Electronics (ISIE), 2014 IEEE 23rd International Symposium on*, 2014, pp. 485-490.
[102] A. F. Cupertino, H. A. Pereira, and V. F. Mendes, "Modeling, Design and Control of a Solar Array Simulator Based on Two-Stage Converters," *Journal of Control, Automation and Electrical Systems*, July 31 2017.
[103] S. Raizada and V. Verma, "Sizing sampling rate of the integrated PV simulator," in *Industrial Electronics and Applications Conference (IEACon), 2016 IEEE*, 2016, pp. 97-103.
[104] J. Chavarría, D. Biel, F. Guinjoan, A. Poveda, F. Masana, and E. Alarcon, "Low cost photovoltaic array emulator design for the test of PV grid-connected

inverters," in *Multi-Conference on Systems, Signals & Devices (SSD), 2014 11th International*, 2014, pp. 1-6.
[105] S. Masashi, Y. Naoki, and I. Muneaki, "Development of Photovoltaic cell emulator using the small scale wind turbine," in *Electrical Machines and Systems (ICEMS), 2012 15th International Conference on*, 2012, pp. 1-4.
[106] A. Algaddafi, N. Brown, R. Gammon, and S. A. Altuwayjiri, "Effect of PV array emulator on power quality of PV inverter compared to a real PV array," in *2015 3rd International Renewable and Sustainable Energy Conference (IRSEC)*, 2015, pp. 1-6.
[107] A. Rachid, F. Kerrour, R. Chenni, and H. Djeghloud, "PV emulator based buck converter using dSPACE controller," in *2016 IEEE 16th International Conference on Environment and Electrical Engineering (EEEIC)*, 2016, pp. 1-6.
[108] Ö. Ö, Y. Duru, S. Zengin, and M. Boztepe, "Design and implementation of programmable PV simulator," in *2016 International Symposium on Fundamentals of Electrical Engineering (ISFEE)*, 2016, pp. 1-5.
[109] S. Thale, R. Wandhare, and V. Agarwal, "A novel low cost portable integrated solar PV, fuel cell and battery emulator with fast tracking algorithm," in *Photovoltaic Specialist Conference (PVSC), 2014 IEEE 40th*, 2014, pp. 3138-3143.
[110] D. W. Hart, *Power Electronics*. Valparaiso University, Indiana: Tata McGraw-Hill Education, 2011.
[111] A. Pressman, *Switching Power Supply Design* vol. 3: McGraw-Hill, Inc., 1997.
[112] M. Ilic and D. Maksimovic, "Interleaved zero-current-transition buck converter," *Industry Applications, IEEE Transactions on,* vol. 43, pp. 1619-1627, 2007.
[113] J. Garcia, A. J. Calleja, D. Gacio Vaquero, and L. Campa, "Interleaved buck converter for fast PWM dimming of high-brightness LEDs," *Power Electronics, IEEE Transactions on,* vol. 26, pp. 2627-2636, 2011.
[114] M. Bendali, C. Larouci, T. Azib, C. Marchand, and G. Coquery, "Design methodology with optimization of an interleaved buck converter for automotive application," in *EUROCON, 2013 IEEE,* 2013, pp. 1066-1072.
[115] Y. Qiu, M. Xu, K. Yao, J. Sun, and F. C. Lee, "Multifrequency Small-Signal Model for Buck and Multiphase Buck Converters," *IEEE Transactions on Power Electronics,* vol. 21, pp. 1185-1192, 2006.
[116] O. García, P. Zumel, A. De Castro, and J. A. Cobos, "Automotive DC-DC bidirectional converter made with many interleaved buck stages," *Power Electronics, IEEE Transactions on,* vol. 21, pp. 578-586, 2006.
[117] Y. Jang, M. M. Jovanovic, and Y. Panov, "Multiphase buck converters with extended duty cycle," in *Proc. IEEE Applied Power Electronics Conf.(APEC'06),* 2006, pp. 38-44.
[118] M. Esteki, B. Poorali, E. Adib, and H. Farzanehfard, "Interleaved Buck Converter With Continuous Input Current, Extremely Low Output Current Ripple, Low Switching Losses, and Improved Step-Down Conversion Ratio," *Industrial Electronics, IEEE Transactions on,* vol. 62, pp. 4769-4776, 2015.
[119] I.-O. Lee, S.-Y. Cho, and G.-W. Moon, "Interleaved buck converter having low switching losses and improved step-down conversion ratio," *Power Electronics, IEEE Transactions on,* vol. 27, pp. 3664-3675, 2012.

[120] M. Cacciato, A. Consoli, G. Scarcella, and A. Testa, "A Multhi-Phase DC/DC Converter for Automotive Dual-voltage Power Systems," *IEEE Industry Applications Magazine,* vol. 40, pp. 2-9, 2004.
[121] M. Esteki, B. Poorali, E. Adib, and H. Farzanehfard, "High step-down interleaved buck converter with low voltage stress," *Power Electronics, IET,* vol. 8, pp. 2352-2360, 2015.
[122] M. K. Kazimierczuk, *Pulse-width Modulated DC-DC Power Converters*. Chichester, West Sussex, PO19 8SQ, United Kingdom: John Wiley and Son, Ltd, 2008.
[123] C.-H. Chang, E.-C. Chang, and H.-L. Cheng, "A high-efficiency solar array simulator implemented by an LLC resonant DC–DC converter," *IEEE Transactions on Power Electronics,* vol. 28, pp. 3039-3046, 2013.
[124] R. D. Cruz and M. Rajesh, "Half bridge LLC resonant DC-DC converter for solar array simulator application," in *2015 International Conference on Technological Advancements in Power and Energy (TAP Energy)*, 2015, pp. 138-143.
[125] R. W. Erickson and D. Maksimovic, *Fundamentals of Power Electronics*, 2 ed. New York, Boston, Dordrecht, London, Moscow: Kluwer Academic Publishers, 2004.
[126] A. Soetedjo, Y. I. Nakhoda, A. Lomi, and G. E. Hendroyono, "Development of PV simulator by integrating software and hardware for laboratory testing," in *2015 International Conference on Automation, Cognitive Science, Optics, Micro Electro-Mechanical System, and Information Technology (ICACOMIT),* 2015, pp. 96-100.
[127] S. Jin, D. Zhang, C. Wang, and Y. Gu, "Optimized Design of Space Solar Array Simulator with Novel Three-port Linear Power Composite Transistor Based on Multiple Cascaded SiC-JFETs," *IEEE Transactions on Industrial Electronics,* vol. PP, pp. 1-1, 2017.
[128] A. Belaout, F. Krim, B. Talbi, H. Feroura, A. Laib, S. Bouyahia, *et al.*, "Development of real time emulator for control and diagnosis purpose of Photovoltaic Generator," in *2017 6th International Conference on Systems and Control (ICSC),* 2017, pp. 139-144.
[129] O. López-Santos, M. C. M. Riveros, M. C. S. Castaño, W. A. Londoño, and G. Garcia, "Emulation of a Photovoltaic Module Using a Wiener-Type Nonlinear Impedance Controller for Tracking of the Operation Point," in *Workshop on Engineering Applications*, 2017, pp. 482-494.
[130] S. Bacha, I. Munteanu, and A. I. Bratcu, *Power Electronic Converters Modeling and Control: with Case Studies* Springer, 2014.
[131] P. Chetty, "Current injected equivalent circuit approach to modeling of switching DC-DC converters in discontinuous inductor conduction mode," *IEEE Transactions on Industrial Electronics,* vol. 3, pp. 230-234, 1982.
[132] V. Vorperian, "Simplified analysis of PWM converters using model of PWM switch. II. Discontinuous conduction mode," *Aerospace and Electronic Systems, IEEE Transactions on,* vol. 26, pp. 497-505, 1990.
[133] G. W. Wester and R. D. Middlebrook, "Low-Frequency Characterization of Switched dc-dc Converters," *Aerospace and Electronic Systems, IEEE Transactions on,* vol. AES-9, pp. 376-385, 1973.
[134] G. Suman, B. V. S. P. Kumar, M. S. Kumar, B. C. Babu, and K. R. Subhashini, "Modeling, Analysis and Design of Synchronous Buck Converter Using State

Space Averaging Technique for PV Energy System," in *Electronic System Design (ISED), 2012 International Symposium on*, 2012, pp. 281-285.

[135] C. Jingquan, R. Erickson, and D. Maksimovic, "Averaged switch modeling of boundary conduction mode DC-to-DC converters," in *Industrial Electronics Society, 2001. IECON '01. The 27th Annual Conference of the IEEE*, 2001, pp. 844-849 vol.2.

[136] S. Cuk and R. D. Middlebrook, "A general unified approach to modelling switching DC-tO-DC converters in discontinuous conduction mode," in *Power Electronics Specialists Conference, 1977 IEEE*, 1977, pp. 36-57.

[137] S. Kasat, "Analysis, Design and Modeling of DC-DC Converter using Simulink," Master of Science, Institute of Engineering and Technology Oklahoma State University 2004.

[138] M. A. Abdullah, C. W. Tan, A. H. Yatim, M. Al-Mothafar, and S. M. Radaideh, "Input current control of boost converters using current-mode controller integrated with linear quadratic regulator," *International Journal of Renewable Energy Research (IJRER),* vol. 2, pp. 262-268, 2012.

[139] D. Chariag and L. Sbita, "Design and simulation of photovoltaic emulator," in *2017 International Conference on Green Energy Conversion Systems (GECS)*, 2017, pp. 1-6.

[140] N. S. Nise, *Control Systems Engineering* vol. 6th Edition. California State Polytechnic University, Pomona WJohn Wiley & Sons, Inc., 2011.

[141] C. P. Ugale and V. V. Dixit, "Buck-boost converter using Fuzzy logic for low voltage solar energy harvesting application," in *2017 11th International Conference on Intelligent Systems and Control (ISCO)*, 2017, pp. 413-417.

[142] J. Lorenzo, J. C. Espiritu, J. Mediavillo, S. J. Dy, and R. B. Caldo, "Development and implementation of fuzzy logic using microcontroller for buck and boost DC-to-DC converter," in *IOP Conference Series: Earth and Environmental Science*, 2017.

[143] B. U. Patil and S. R. Jagtap, "Adaptive fuzzy logic controller for buck converter," in *2015 International Conference on Computation of Power, Energy, Information and Communication (ICCPEIC)*, 2015, pp. 0078-0082.

[144] S. Vinod, M. Balaji, and M. Prabhakar, "Robust control of parallel buck fed buck converter using hybrid fuzzy PI controller," in *2015 IEEE 11th International Conference on Power Electronics and Drive Systems*, 2015, pp. 347-351.

[145] C. S. Betancor-Martin, J. Sosa, J. A. Montiel-Nelson, and A. Vega-Martinez, "Gains tuning of a PI-Fuzzy controller by genetic algorithms," *Engineering Computations (Swansea, Wales),* vol. 31, pp. 1074-1097, 2014.

[146] M. C. Di Piazza and G. Vitale, "Photovoltaic field emulation including dynamic and partial shadow conditions," *Applied Energy,* vol. 87, pp. 814-823, 3// 2010.

[147] S. Jin, D. Zhang, and C. Wang, "UI-RI Hybrid Lookup Table Method with High Linearity and High-Speed Convergence Performance for FPGA-based Space Solar Array Simulator," *IEEE Transactions on Power Electronics,* 2017.

[148] I. D. G. Jayawardana, C. N. M. Ho, M. Pokharel, and G. Escobar, "A fast dynamic photovoltaic simulator with instantaneous output impedance matching controller," in *2017 IEEE Energy Conversion Congress and Exposition (ECCE)*, 2017, pp. 5126-5132.

[149] H. Nagayoshi, "Characterization of the module/array simulator using IV magnifier circuit of a pn photo-sensor," in *Photovoltaic Energy Conversion, 2003. Proceedings of 3rd World Conference on,* 2003, pp. 2023-2026.
[150] H. Nagayoshi, S. Orio, Y. Kono, and H. Nakajima, "Novel PV array/module I-V curve simulator circuit," in *Photovoltaic Specialists Conference, 2002. Conference Record of the Twenty-Ninth IEEE*, 2002, pp. 1535-1538.
[151] P. Wei, B. Tan, H. Zhang, and Y. Zhao, "Research on maximum power point tracker based on solar cells simulator," in *Advanced Computer Control (ICACC), 2010 2nd International Conference on*, 2010, pp. 319-323.
[152] A. K. Mukerjee and N. Dasgupta, "DC power supply used as photovoltaic simulator for testing MPPT algorithms," *Renewable Energy,* vol. 32, pp. 587-592, 4// 2007.
[153] L. A. Lopes and A.-M. Lienhardt, "A simplified nonlinear power source for simulating PV panels," in *Power Electronics Specialist Conference, 2003. PESC'03. 2003 IEEE 34th Annual*, 2003, pp. 1729-1734.
[154] Z. Zhou and J. Macaulay, "An Emulated PV Source Based on an Unilluminated Solar Panel and DC Power Supply," *Energies*, vol. 10, p. 2075, 2017.
[155] M. Ünlü and S. Çamur, "Solar irradiance emulator based on DC power supply for photovoltaic panels," in *2017 9th International Conference on Electronics, Computers and Artificial Intelligence (ECAI)*, 2017, pp. 1-4.
[156] M. Ünlü and S. Çamur, "A simple Photovoltaic simulator based on a one-diode equivalent circuit model," in *2017 4th International Conference on Electrical and Electronic Engineering (ICEEE)*, 2017, pp. 33-36.
[157] H. B. Mustafa, "Design and Control Of A Photovoltaic Simulator," Bachelor of Electrical Engineering, Department of Electrical Power Engineering, Universiti Teknologi Malaysia, Skudai, Johor, Malaysia, 2016.
[158] A. Solar, "Ameresco Solar 80W (24V) Photovoltaic Modules - 80J-B (24V)," ed: Ameresco Inc., 2014.
[159] R. Kadri, H. Andrei, J.-P. Gaubert, T. Ivanovici, G. Champenois, and P. Andrei, "Modeling of the photovoltaic cell circuit parameters for optimum connection model and real-time emulator with partial shadow conditions," *Energy,* vol. 42, pp. 57-67, 6// 2012.
[160] R. Sedgewick and K. Wayne, *Algorithms*, 4th Edition ed. Boston, Massachusetts: Pearson Education, 2011.
[161] N. Shiota, V. Phimmasone, T. Abe, and M. Miyatake, "A MPPT algorithm based on the binary-search technique with ripples from a converter," in *2013 International Conference on Electrical Machines and Systems (ICEMS)*, 2013, pp. 1718-1721.
[162] A. Marquez, J. I. Leon, S. Vazquez, L. G. Franquelo, J. M. Carrasco, and E. Galvan, "Binary search based MPPT algorithm for high-power PV systems," in *2016 10th International Conference on Compatibility, Power Electronics and Power Engineering (CPE-POWERENG)*, 2016, pp. 168-173.
[163] C. T. Phan-Tan and N. Nguyen-Quang, "A P&O MPPT method for photovoltaic applications based on binary-searching," in *2016 IEEE International Conference on Sustainable Energy Technologies (ICSET)*, 2016, pp. 78-82.
[164] Panasonic, "EEUFR1J180B - Electrolytic Capacitor, 18 µF, 63 V, FR Series, ± 20%, Radial Leaded, 5 mm," ed: PANASONIC ELECTRONIC COMPONENTS.

[165] Bourns, "1140-182K-RC - High Current Choke, 1.8MH, 4.5A 10%," B. J. Miller, Ed., ed. Bourns JW Miller, 2014.
[166] O. Semiconductor, "IRF644B N-Channel BFET MOSFET 250 V, 14 A, 280 mOhm," O. Semiconductor, Ed., ed, 2013.
[167] IXYS, "DSEI30-10A - Fast / Ultrafast Diode, 1 kV, 30 A, Single, 2.4 V, 35 ns, 200 A," ed: IXYS SEMICONDUCTOR, 1997.
[168] S. Srivastava, Y. Kumar, A. Misra, S. K. Thakur, and V. S. Pandit, "Optimum design of buck converter controller using LQR approach," in *2013 15th International Conference on Advanced Computing Technologies (ICACT)*, 2013, pp. 1-6.
[169] M. C. D. Piazza and G. Vitale, *Photovoltaic Sources: Modeling and Emulation*. Verlag, London, United Kingdom: Springer, 2013.
[170] J. Ahmed and Z. Salam, "An improved perturb and observe (P&O) maximum power point tracking (MPPT) algorithm for higher efficiency," *Applied Energy*, vol. 150, pp. 97-108, 7/15/ 2015.
[171] M. T. Outeiro, G. Buja, and D. Czarkowski, "Resonant Power Converters: An Overview with Multiple Elements in the Resonant Tank Network," *IEEE Industrial Electronics Magazine*, vol. 10, pp. 21-45, 2016.
[172] Ferroxcube, "Ferroxcube ETD49/25/16-3C95 114 mm, 211 mm²," ed: Ferroxcube A Yageo Company, 2008.
[173] Vishay, "MAL215262479E3 - Electrolytic Capacitor, 47 µF, 200 V, 152 RMH Series, ± 20%, Radial Leaded, 12.5 mm," ed, 2012.
[174] LEM, "Current Tranducer LEM HY 5..25-P/SP1 Version 9," ed, 2014.
[175] LEM, "Voltage Tranducer LV 25-P," ed, 2014.
[176] X. POWER, "IH0515S - 2 Watt SIP Dual Output DC/DC Converter, Input 5V, Output ±15V/66mA," X. POWER, Ed., ed, 2017.
[177] T. L. Floyd, *Electronic Devices*, 9th Edition ed. Prentice Hall, 1 Lake Street, Upper Saddle River, New Jersey: Pearson, 2012.
[178] X. POWER, "IA0509S - 1 Watt DIP Single Output DC/DC Converter, Input 5V, Output 9V/55mA," X. POWER, Ed., ed, 2017.